

# Superspreading events suggest aerosol transmission of SARS-CoV-2 by accumulation in enclosed spaces

John M. Kolinski<sup>1</sup> & Tobias M. Schneider<sup>1</sup>

<sup>1</sup>*Institute of Mechanical Engineering, École Polytechnique Fédérale de Lausanne, Lausanne, 1015, Switzerland*

**Viral transmission pathways have profound implications for public safety; thus it is imperative to establish an accurate and complete understanding of viable infectious avenues.** Whether SARS-CoV-2 is airborne is currently uncertain<sup>1,2</sup>. While mounting evidence suggests it could be transmitted via the air in confined spaces<sup>3,4</sup>, the airborne transmission mode has not yet been demonstrated. Here we show that the quantitative analysis of several reported superspreading events points towards aerosol mediated transmission of SARS-CoV-2. Aerosolized virus emitted by an infected person in an enclosed space will accumulate until virion emission and virion destabilization are balanced, resulting in a steady-state concentration  $C_\infty$ . The timescale to accumulation leads to significantly enhanced exposure when virus-carrying aerosol droplets are inhaled for longer duration co-occupancy. Reported superspreading events are found to trace out a single value of the calculated virion exposure, suggesting a universal minimum infective dose (MID) via aerosol. The MID implied by our analysis is comparable to the measured MIDs for influenza A (H2N2)<sup>5,6</sup>, the virus responsible for the 1957-1958 asian flu pandemic. Our model suggests that the likelihood for aerosol-mediated transmission reduces significantly when there is filtration at a rate exceeding the

## **destabilization rate of aerosolized SARS-CoV-2.**

The infectious pathways of a virus determine its course as it infects a host population. Despite clear guidelines on social distancing and lock-down policies<sup>7</sup>, SARS-CoV-2 has proven to be an extremely challenging virus to successfully contain due in part to its prolonged symptomless incubation period<sup>8,9</sup>. Mask-wearing has proven to be marginally effective in reducing viral transmission<sup>10</sup>, but not all infectious particles are captured by typical surgical masks<sup>11</sup>. Whether a virus is transmitted is fundamentally governed by the virus shedding rate of the infected person, the minimal infective dose (MID) necessary to cause an infection and the transmission pathway mediating virus material delivery to a potential host.

The pathway for transmission of respiratory viruses via droplets depends on their size, as depicted schematically in Fig.1 a. For small droplets with radius  $a$  below 5 microns settling in quiescent air, the gravitational force  $F_g = 4/3 \pi \rho g a^3$ , is balanced by Stokes drag acting on the droplet,  $F_d = 6\pi a \mu v$ . The droplet thus descends at a velocity  $v$  of 3 meters per hour. Prevailing currents in a typical room driven by convection, active ventilation or movement of people significantly exceed this settling velocity. Consequently, aerosolized droplets will remain suspended for hours, dispersing widely in an occupied room within minutes<sup>3,12</sup>. Because aerosolized droplets remain in suspension long enough to thoroughly mix, the physical distance between persons in an enclosed space becomes irrelevant; exposure to the airborne virus is controlled only by the concentration of virus particles in the air. This is in contrast to large respiratory droplet transmission. Indeed, a droplet's settling velocity increases quadratically with its radius, so that large droplets

only remain suspended for seconds before they fall to the ground, leading to a limited spatial range of infectivity<sup>13-15</sup>, and serving as motivation for the current social distancing guidelines. Here we consider virus transport by small aerosol-sized droplets only. Direct measurements of hospital air have identified SARS-CoV-2 material in aerosols<sup>16</sup>, but exposed healthcare workers in hospital environments were not infected<sup>1,2</sup>, casting doubt on the airborne transmission pathway despite demonstrable viral content in aerosol form.

The viral titer of SARS-CoV-2, or the concentration of infectious viral particles, has been shown to decay exponentially in air at a timescale of one hour for SARS-CoV-2<sup>17</sup>. The aerosol emission rate of infected persons is believed to vary widely between infected persons. Under typical conditions, the aerosol emission rate of some persons infected with other types of corona viruses was measured to exceed 10,000 viral particles in a half-hour period, with the majority of infected persons emitting no measurable aerosol virus<sup>18</sup>. As we will show, infected persons shedding via aerosol at average rates have the potential to trigger superspreading events.

Exposure to the virus does not ensure that it will successfully infect, as a virus must first cross the body's protective barriers. Known viruses are infectious at various exposure thresholds, or minimum infective doses (MIDs), as low as a few hundred viral particles in the case of influenza A (H2N2) and SARS-CoV-1<sup>5,6</sup>. More virulent diseases can even infect at substantially lower exposures<sup>5</sup>. Such a threshold likely exists for SARS-CoV-2<sup>6</sup>, though it has yet to be determined.

No airborne transmission of SARS-CoV-2 was detected among exposed medical workers in a hospital environment<sup>1,2</sup>; however, hospitals typically have strong requirements for air refreshment

and filtration that do not apply to gyms or bars. Indeed, low air refreshment rates facilitate the accumulation of virions, which are neither expelled nor filtered from the environment<sup>3,19</sup>. To study the effect of virus accumulation in such environments, we use straightforward conservation laws of aerosol-born virions to formulate an expression for the time-rate-of-change of the volumetric concentration of virus particles in aerosol form  $C(t)$  at time  $t$  in terms of a viral source  $s$ , in number of aerosol-born viral particles shed per time, and a destabilization rate  $\gamma$ , the fraction of viral particles in aerosol that lose their virality per unit time, as  $\frac{dC(t)}{dt} = s/V - \gamma C(t)$ . Here  $V$  is room volume. If the room air is filtered or replenished, a third term  $\gamma_{filt}C(t)$  is subtracted from the right-hand side of this equation yielding an effective destabilization rate that combines the natural decay and filtration. The effect of filtration on aerosolized SARS-CoV-2 concentration is presented in Fig. 1 of the extended material.

We assume that the flow within the room under consideration is well-mixed within minutes; this is fast compared to  $1/\gamma$ , which is 1 hour for SARS-CoV-2<sup>17</sup>. Because the air is well mixed, the complex spatio-temporal evolution of aerosol distribution can be represented by the uniform virion concentration  $C(t)$ , which is a function of time only. We depict this scenario schematically in Fig. 1 a. The expression  $C(t) = \frac{s}{\gamma V}(1 - e^{-\gamma t})$  describes the temporal evolution of  $C$ , as shown in Fig. 1 b.

While the viral shedding rate for SARS-CoV-2 has not yet been measured, the shedding rate of other corona viruses has been measured at over 20,000 virions / hour<sup>18</sup>. Among a group of aerosol-shedding virus-positive persons, the average number of virions shed per hour was  $s =$

32,600 virions / hour. We use this value for  $s$  throughout this study, as described in Methods. We can now calculate the steady-state concentration of virions  $C_\infty$  for an infectious person in a room of a given size. A single infected person shedding aerosolized virus in a large room of 300 cubic meters yields  $C_\infty = 109$  virions/m<sup>3</sup>, while in a smaller space of 40 cubic meters gives a much larger  $C_\infty = 814$  virions/m<sup>3</sup>. This steady-state concentration is reached after a transient period given by the inverse destabilization rate of the virus; since  $\gamma$  is 1/hour, short-term occupancy is unlikely to reach the steady-state concentration, significantly reducing virion exposure in transient encounters.

Is an occupant likely to be infected at such concentrations? To answer this question, we calculate the virion exposure  $N_{exp}$ , recognizing that it must exceed a minimum infective dose (MID).  $N_{exp}$  is given by the time-integral of the respiration rate of a room occupant,  $\dot{Q}$ , as  $N_{exp} = \int_0^T C(t)\dot{Q}dt$ , where  $\dot{Q}$  is the respiration rate. The average adult at rest takes 12 breaths per minute, cycling a volume of 0.5 liters / breath; this amounts to a total respiration rate of 360 liters per hour, or  $\dot{Q} = 0.36m^3 / hour$ . Thus,  $N_{exp}$  with a single infected occupant in the above cases is 14 and 108 per hour, respectively. We see the pronounced effect of the approach to steady-state when we evaluate  $N_{exp}$  for 30 minutes: it is 4 and 31 particles, respectively; thus it is less than 1/3 the exposure for twice that time period.

The minimum infectious dose (MID) for aerosolized SARS-CoV-2 is currently unknown; however, other viruses provide a guide for estimating this value. The MID of human respiratory viruses varies greatly and depends on the infection pathways. Very infectious viruses including

the aggressive Influenza A (H2N2), adenoviruses and SARS-CoV-1, fall between several tens to several hundreds of virions<sup>5,6,20</sup>. We note that  $N_{exp}$  exceeds 50 in under 40 minutes for the  $40\ m^3$  room, but it takes over 2 hours for  $N_{exp}$  to exceed 50 in the  $300\ m^3$  room; thus, the likelihood of infection depends strongly on room volume. This analysis can be generalized for arbitrary times and room volumes; we present several iso- $N_{exp}$  curves as a function of time and room volume in Fig. 2. Regrettably, at room volumes that are typically encountered in daily activities, and over timescales of co-occupancy of the order of hours, we observe iso- $N_{exp}$  values that fall within the range of the MIDs reported for other aerosol-transmissible viruses<sup>5,6</sup>.

The model together with reasonable estimates for parameter values yields exposure doses compatible with minimum infective doses reported for other aerosol-transmissible viruses and thus suggests that airborne transmission of SARS-CoV-2 is possible. To assess the viability of aerosolized SARS-CoV-2 transmission despite unknown minimal infective dose information, we analyse reported super-spreading events. For each dataset used in our analysis, the number of viral shedders is known, the room volume is reported or easily estimated using available data, and identical co-occupancy time is documented. In order to isolate the effects of aerosol transmission from the more common pathway of direct contact or ballistic droplets, the interactions should predominantly take place between non-related persons, where close proximal interaction is less likely. These requirements are met for several well-documented superspreading events<sup>21-24</sup>, in particular for a lunch period at a restaurant<sup>24</sup>, where CCTV footage documented the non-interaction between adjacent persons and tables, thus underscoring the importance of the aerosol transmission mechanism. Furthermore, a superspreading event reported at a meat processing plant in Germany

took place *after* strict social distancing and hygiene measures were put in place, strictly suppressing the pathway for SARS-CoV-2 infection via close physical contact<sup>25</sup>. Each of these events is documented, and the rationale for parameter values is annotated, in Methods.

We now compare the room volume and co-occupancy time for the sub-set of events that involve a single viral shedder at a resting respiratory rate, corresponding to the parameter values used to calculate the iso- $N_{exp}$  in Fig. 2. Among the five events with a single identified virus shedder at the resting respiration rate, the data fall within a remarkably consistent range of  $N_{exp}$  between 50 and 100, as shown in Fig. 2. This tight range of  $N_{exp}$  that leads to super-spreading events suggests a possible unique MID via aerosol transmission for SARS-CoV-2 of  $N_{exp} \approx 50$ .

If the value of  $N_{exp} \approx 50$  is indeed the MID for aerosol transmission of SARS-CoV-2, it should independently arise under further analysis. We test this hypothesis by extending our analysis to other super-spreading events with identical co-occupancy with different respiration rates<sup>22</sup> or number of spreaders<sup>23</sup>. Using the same analysis framework, but accounting for these modifications of source number or respiration rate as described in the extended material<sup>7</sup>, we tabulate and graph the predictions of  $N_{exp}$ , along with the data plotted in Figure 2. We find that with the exception of two events that involve documented close physical contact<sup>23,26</sup>, all cases fall within the anticipated range of  $N_{exp} \approx 50$  virions, as can be seen in Fig. 3.

Using a simple mathematical model for virion accumulation and exposure, we find that several superspreading events involving over 100 infections with SARS-CoV-2 suggest the same range of minimal infective dose of  $N_{exp} \approx 50$  virions. The accumulation dynamics emphasize the im-

portance of transient behavior, as has been previously identified in studies of store occupancy in Italy<sup>19</sup> using a similar mathematical framework.

Our model is built upon two key parameters: first, the rate of virion shedding by an infected person<sup>18</sup>, and second the virion destabilization rate<sup>17</sup>. We additionally assume that filtration is slow compared to the viral destabilization rate. However, this framework also emphasizes the importance of filtration as we present in detail in extended material Fig. 1<sup>7</sup>. If the volumetric exchange of air is greater than one or two room volumes per hour,  $C_\infty$  can be reduced by a factor of two. In hospital environments, where the air filtration rate can exceed 10 volumes per hour, our model suggests that  $N_{exp}$  over several hours can be reduced approximately 10-fold. Such a reduction would potentially reduce  $N_{exp}$  below the MID for SARS-CoV-2. This might explain why exposed medical workers in a hospital environment were not infected<sup>1,2</sup>.

Within the framework of aerosol transmission by accumulation, superspreading events suggest minimum infective doses of SARS-CoV-2 commensurate with other infectious viruses, including the influenza-A (H2N2) strand that caused the 1957-'58 influenza pandemic<sup>5,6</sup>. Indeed, our study suggests that in terms the infective dose for aerosolized transmission, SARS-CoV-2 behaves much like a particular flu - unfortunately, the H2N2 flu strand that generated a global pandemic. The evidence for the potential airborn transmission for SARS-CoV-2 is by now sufficient to form a scientific consensus<sup>3,4,12</sup>; however, the significance of this transmission mode has not yet been directly demonstrated. Under the condition that virions are transported by aerosol droplets, data from several reported superspreading events all indicate the same narrow range of infectious

dose. This points towards the practical relevance of aerosol transmission of SARS-CoV-2.

## Methods

**Determination of parameter values.** There are 3 primary parameters that are used to calculate  $N_{exp}$ :  $s$ ,  $\dot{Q}$  and  $\gamma$ .  $s$  represents the source strength in units of aerosolized virions per hour,  $\dot{Q}$  is the respiratory volume per hour and  $\gamma$  is the proportion of aerosolized viruses that destabilize in one hour.

$s$  is currently unknown for SARS-CoV-2. In order to constrain this parameter, we evaluate the number of virions emitted per hour on average for three other human corona viruses: HCoV-NL63, HCoV-OC43 and HCoV-HKU1<sup>18</sup>. Within the sampling of these viruses, all three were represented in aerosol shedding, and a total of 4 of 10 total infected persons shed aerosolized virus in this study<sup>18</sup>. The number of virions shed varied from 660 to 57,000 in 1/2 hour; 16,300 were shed on average, corresponding to an average value of  $s = 32,600$  virions / hour. This value of  $s$  is used throughout the manuscript. Notably,  $s$  might vary depending on the activity reported - for example, singing<sup>21</sup> or exercise<sup>22</sup> might augment the value of  $s$ ; as we have no way of determining how  $s$  could vary under these circumstances, we retain the same value in all calculations. It is furthermore interesting to note that both the aerosol virus shedding rates, and the fraction of infected persons shedding aerosolized virus, are commensurate for three analyzed corona viruses and two influenza viruses<sup>18</sup>, suggesting that there could be similarities between these families of viruses, as was previously noted<sup>6</sup>.

The respiratory rate  $\dot{Q}$  for an adult person is known to be 12 breaths per hour, and the volume per breath is 0.5 liters on average. This corresponds to  $\dot{Q} = 0.36 \text{ m}^3 / \text{hour}$ ; this value is used for

all calculations except the high-intensity fitness class<sup>22</sup>, where an elevated  $\dot{Q} = 1.08 \text{ m}^3 / \text{hour}$  is used, corresponding to a three-fold higher respiratory rate.

$\gamma$  was extracted directly from data collected for aerosolized SARS-CoV-2<sup>17</sup>. In a one hour period, the viral titer drops by approximately  $e^{-1}$ , setting  $\gamma = 1 / \text{hour}$ . A second study suggested that aerosolized virus can remain infectious for a far longer period<sup>27</sup>; however, these data do not convey a convincing trend, and the data are significantly less dense than in the study used here to determine  $\gamma$ <sup>17</sup>.

**Obtaining values for  $V$ ,  $T$  and number of shedders** The formulation of our model requires an accurate determination of the room volume  $V$ , the co-occupancy period  $T$  and the number of aerosol-based virion shedders to calculate  $N_{exp}$ . While some studies report these values, for example by including full spatial maps of the environment<sup>25</sup>, others report partial data for  $V$  without the room height<sup>22,24</sup>, or no data at all for  $V$  other than a venue description<sup>21,23</sup>. Typically, values for  $T$  were very well constrained, including co-occupancy times down to the minute, recorded with CCTV footage of the incident in one case<sup>24</sup>. In total, the data collected comprise 20 discrete events, with all but the fitness class comprising a single event. The fitness classes involved 12 different events, driven by the simultaneous infection of several fitness class instructors at a training event prior to the several classes held in the following week<sup>22</sup>. The data evaluated in this manuscript correspond to a total of 207 infections with over 1100 documented persons exposed.

There was typically a single documented infector for the superspreading events analyzed here. For the tour group, there were likely two infectors from a co-travelling sub-group of a 20

person tour (cluster A)<sup>23</sup>. A single infector is most likely for all the other events, although the morning shift workers at the German meat processing facility were exposed by a primary infector who worked and lived with a potential secondary infector (labeled B1 and B2), where the first co-exposure took place on the day prior to the three days of total exposure during shift work<sup>25</sup>. The Jordanian wedding event was triggered by a primary source who had close contact with a large number of participants in two days prior to the two hour wedding, and likely had close contact with a large number of attendees during the wedding itself, as the primary source was the bride's father<sup>26</sup>; as such, non-aerosol pathways cannot be ruled out and are indeed likely to have contributed to the scale of the outbreak. A short duration encounter with two sources in Singapore also included close inter-personal contact at a health products shop, where interactions likely took place via person to person contact (cluster A, health products shop)<sup>23</sup>; thus, also in this event non-aerosol mediated infection is likely.

Values for  $V$  were reported directly<sup>25</sup>, calculated from the reported floor area<sup>22,24</sup> with an estimated ceiling height range, or estimated / calculated from alternative sources<sup>21,23,26</sup>. For the German meat processing facility the full dimensions of the shared shift space were provided; we used only the proximal floor space in our analysis, as walls separated this volume from the remainder of the plant<sup>25</sup>. The Jordanian wedding took place at an indoor facility designed to accommodate approximately 400 guests<sup>26</sup>; estimating approximately  $16 \text{ m}^2$  per 10 persons yields a floor area of approximately  $640 \text{ m}^2$ ; with a room height of 3 to 5 meters, we obtain a volume estimate of approximately  $2600 \pm 700 \text{ m}^3$ . Similar considerations were used to determine the size of the conference dinner facility in cluster B for a total of 100 conference attendees<sup>23</sup>. The choral practice

event took place in Skagit county, Washington<sup>21</sup>. The choir's website provides photos of the choral practice room prior to the outbreak, enabling measurements of the floor area with an uncertainty of a few meters per dimension<sup>28</sup>. Neither the jewelry store, the health products shop, nor the church included values of  $V$  or floor space<sup>23</sup>; in each of these cases, between 5 and 10 google street view images of stores belonging to these categories were analyzed, and appropriately wide error bounds were used for  $V$ . The Korean fitness class events reported a room size of approximately 60 m<sup>222</sup>, and a floorplan was provided for the Chinese restaurant lunch<sup>24</sup>. In both cases, room heights were not provided and are estimated between 3 and 4 meters. For the Chinese restaurant lunch, the total restaurant area was served by two primary air conditioners. We selected the zone of the restaurant served by the air conditioner where the infected person sat, as this was a distinct zone within the restaurant<sup>24</sup>.

The period of co-occupancy  $T$  was reported in either minutes or fractions of an hour, and is thus tightly constrained for each event. For the German meat processing plant, three morning shifts over a span of three days were reported as exposed. A total of two hours of breaks were reported during these shifts; thus we use a 6 hour period per shift<sup>25</sup>. The total period of exposure thus constitutes 18 hours. In our analysis, we explicitly ignore any effects outside of these shifts including metabolism or decay of virions during off hours, for example.

The number of superspreading events we analyze is not comprehensive, as there are significantly more superspreading events that have been identified in the literature; however, it is not common practice to include the precise size of the space, or even the time duration of the interaction, and thus these events are excluded from this analysis. Furthermore, a significantly number

of better documented superspreading events were clearly associated with close inter-personal contact (e.g. families, roommates, etc.) and thus are not compatible with the analytical framework presented here.

1. Faridi, S. *et al.* A field indoor air measurement of SARS-CoV-2 in the patient rooms of the largest hospital in Iran. *Sci. Total Environ.* **725**, 138401 (2020).
2. Cheng, V. C.-C. *et al.* Air and environmental sampling for SARS-CoV-2 around hospitalized patients with coronavirus disease 2019 (COVID-19). *Infect. Control Hosp. Epidemiol.* 1–8. <https://www.ncbi.nlm.nih.gov/pmc/articles/pmc7327164/> (2020).
3. Morawska, L. & Cao, J. Airborne transmission of SARS-CoV-2: The world should face the reality. *Environ. Int.* **139**, 105730 (2020).
4. Fennelly, K. P. Particle sizes of infectious aerosols: implications for infection control. *Lancet Resp. Med.* <https://linkinghub.elsevier.com/retrieve/pii/s2213260020303234> (2020).
5. Yezli, S. & Otter, J. A. Minimum Infective Dose of the Major Human Respiratory and Enteric Viruses Transmitted Through Food and the Environment. *Food Environ. Virol.* **3**, 1–30 (2011).
6. Schrder, I. COVID-19: A Risk Assessment Perspective. *ACS Chem. Health Saf.* **27**, 160–169 (2020).
7. Advice for the public on COVID-19 World Health Organization. <https://www.who.int/emergencies/diseases/novel-coronavirus-2019/advice-for-public> (2020).

8. Chu, H. *et al.* Comparative Replication and Immune Activation Profiles of SARS-CoV-2 and SARS-CoV in Human Lungs: An Ex Vivo Study With Implications for the Pathogenesis of COVID-19. *Clin. Infect. Dis.* <https://academic.oup.com/cid/advance-article/doi/10.1093/cid/ciaa410/5818134> (2020).
9. Furukawa, N. W., Brooks, J. T. & Sobel, J. Evidence Supporting Transmission of Severe Acute Respiratory Syndrome Coronavirus 2 While Presymptomatic or Asymptomatic. *Emerg. Infect. Dis.* **26** (2020). [http://wwwnc.cdc.gov/eid/article/26/7/20-1595\\_article.htm](http://wwwnc.cdc.gov/eid/article/26/7/20-1595_article.htm) (2020).
10. Zhang, R., Li, Y., Zhang, A. L., Wang, Y. & Molina, M. J. Identifying airborne transmission as the dominant route for the spread of COVID-19. *Proc. Natl. Acad. Sci. USA* **117**, 14857–14863 (2020).
11. Khler, C. J. & Hain, R. Fundamental protective mechanisms of face masks against droplet infections. *J. Aerosol Sci.* **148**, 105617 (2020).
12. Prather, K. A., Wang, C. C. & Schooley, R. T. Reducing transmission of SARS-CoV-2. *Science* **368**, 1422–1424 (2020).
13. Bourouiba, L. Turbulent Gas Clouds and Respiratory Pathogen Emissions: Potential Implications for Reducing Transmission of COVID-19. *JAMA* **323** (2020).
14. Mittal, R., Ni, R. & Seo, J.-H. The flow physics of COVID-19. *J. Fluid Mech.* **894**, F2 1–14 (2020).
15. Somsen, G. A., van Rijn, C., Kooij, S., Bem, R. A. & Bonn, D. Small droplet aerosols in poorly ventilated spaces and SARS-CoV-2 transmission. *Lancet Resp. Med.* **8**, 658–659 (2020).

16. Liu, Y. *et al.* Aerodynamic analysis of SARS-CoV-2 in two Wuhan hospitals. *Nature* **582**, 557–560 (2020).
17. van Doremalen, N. *et al.* Aerosol and Surface Stability of SARS-CoV-2 as Compared with SARS-CoV-1. *New Engl. J. Med.* **382**, 1564–1567 (2020).
18. Leung, N. H. L. *et al.* Respiratory virus shedding in exhaled breath and efficacy of face masks. *Nat. Med.* **26**, 676–680 (2020).
19. Buonanno, G., Stabile, L. & Morawska, L. Estimation of airborne viral emission: Quanta emission rate of SARS-CoV-2 for infection risk assessment. *Environ. Int.* **141**, 105794 (2020).
20. Watanabe, T., Bartrand, T. A., Weir, M. H., Omura, T. & Haas, C. N. Development of a Dose-Response Model for SARS Coronavirus. *Risk Anal.* **30** (2010).
21. Hamner, L. *et al.* High SARS-CoV-2 Attack Rate Following Exposure at a Choir Practice Skagit County, Washington, March 2020. *MMWR-Morbid. Mortal. W.* **69**, 606–610 (2020).
22. Jang, S., Han, S. H. & Rhee, J.-Y. Cluster of Coronavirus Disease Associated with Fitness Dance Classes, South Korea. *Emerg. Infect. Dis.* **26**, 1917–1920 (2020).
23. Pung, R. *et al.* Investigation of three clusters of COVID-19 in Singapore: implications for surveillance and response measures. *Lancet* **395**, 1039–1046 (2020).
24. Lu, J. *et al.* COVID-19 Outbreak Associated with Air Conditioning in Restaurant, Guangzhou, China, 2020. *Emerg. Infect. Dis.* **26**, 1628–1631 (2020).

25. Gnther, T. *et al.* Investigation of a superspreading event preceding the largest meat processing Preprint at [https://papers.ssrn.com/sol3/papers.cfm?abstract\\_id=3654517](https://papers.ssrn.com/sol3/papers.cfm?abstract_id=3654517) (2020).
26. Yusef, D. *et al.* Large Outbreak of Coronavirus Disease among Wedding Attendees, Jordan. *Emerg. Infect. Dis.* **26**. [https://wwwnc.cdc.gov/eid/article/26/9/20-1469\\_article](https://wwwnc.cdc.gov/eid/article/26/9/20-1469_article) (2020).
27. Fears, A. C. *et al.* Persistence of Severe Acute Respiratory Syndrome Coronavirus 2 in Aerosol Suspensions. *Emerg. Infect. Dis.* **26**. [https://wwwnc.cdc.gov/eid/article/26/9/20-1806\\_article](https://wwwnc.cdc.gov/eid/article/26/9/20-1806_article) (2020).
28. Skagit county chorale <https://www.skagitvalleychorale.org/> (2020).

**Competing Interests** The authors declare that they have no competing financial interests.

**Correspondence** Correspondence and requests for materials should be addressed to J.M.K. (email: [john.kolinski@epfl.ch](mailto:john.kolinski@epfl.ch)) or T.M.S. (email: [tobias.schneider@epfl.ch](mailto:tobias.schneider@epfl.ch)).

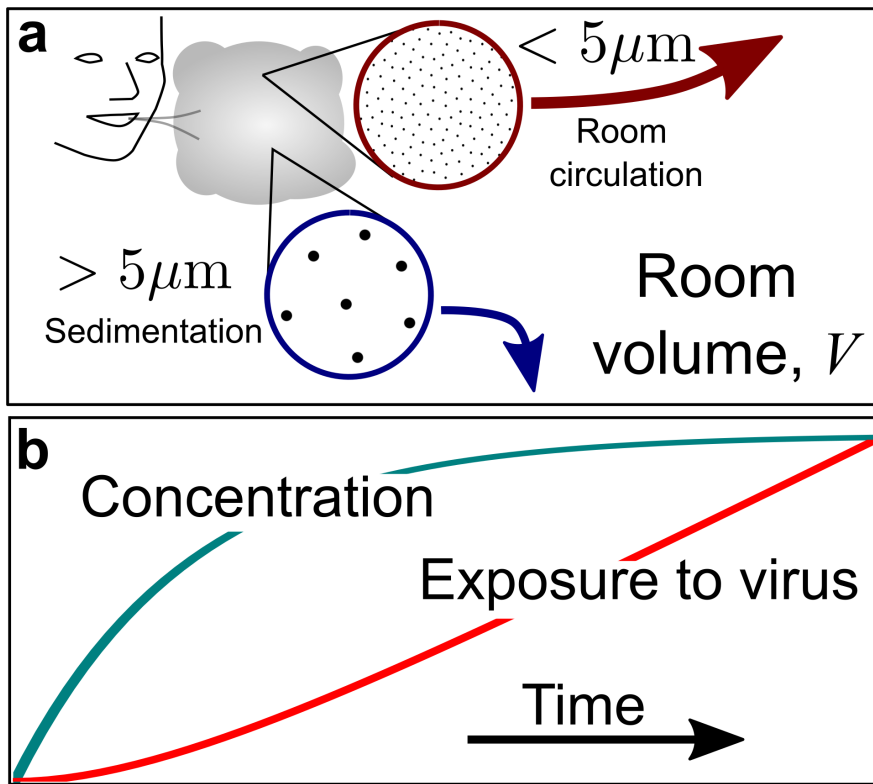


Figure 1: Aerosolization of viral cargo in an enclosed space. a) A schematic of a closed room with volume  $V$ . An infected person can emit *both* rapidly sedimenting respiratory droplets and aerosol-sized particles when breathing, speaking, coughing or sneezing. Particles with a diameter of 5  $\mu\text{m}$  sediment in quiescent air at a rate of 3 m/hour. These particles are readily dispersed by room currents set up by air conditioning, thermal gradients and background flow of the room air. b) For aerosolized virus emitted into an enclosed space, the rate of emission will ultimately be balanced by the destabilization rate; these dynamics lead to the evolution of aerosolized virus concentration plotted here. A non-infected occupant breathing at a constant rate in the same space is exposed to  $N_{exp}$  particles over time (right axis).

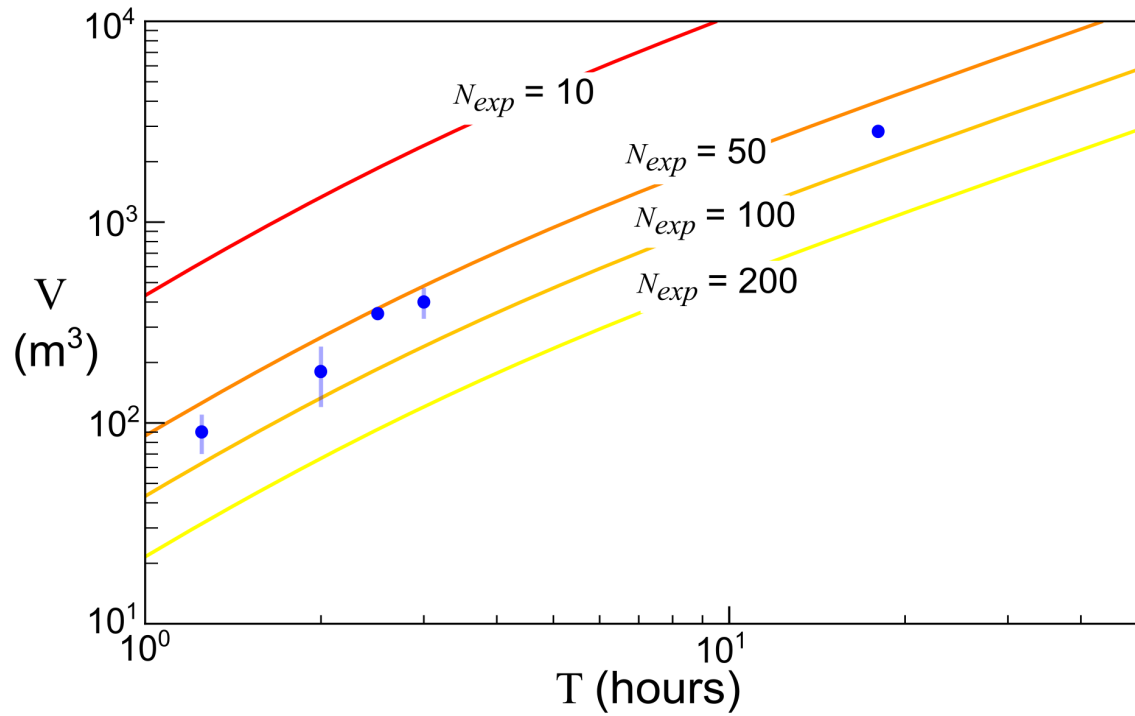
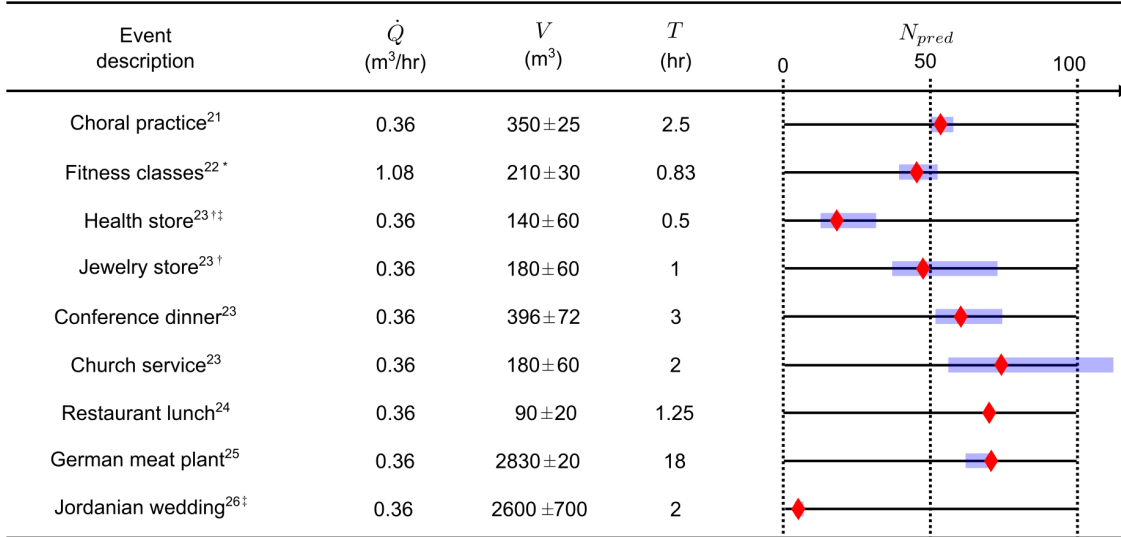


Figure 2: Curves of constant aerosolized virion exposure for a fixed source strength and breathing rate.  $N_{exp}$ , the number of viral particles a room occupant is exposed to, is calculated as a function of room volume  $V$  and occupancy time  $T$ .  $N_{exp}$  is indicated on each curve. Data from several super-spreading events<sup>21,23–25</sup> with a single spreading source in non-exercise scenarios are plotted on the graph, with error bars indicated for the events. Details of these events, and assumptions used in the calculation of the iso- $N_{exp}$  curves are included in Methods.



\*The respiratory rate at the fitness class is taken to be three times larger than the resting respiratory rate.

†The number of infectors is two, and not one for these events.

‡Close personal contact is specifically cited in both of these events.

Figure 3: Tabulated data for several super-spreading events. A total of 20 distinct superspreading events<sup>21–26</sup> for SARS-CoV-2 are analyzed, and the parameter values used to formulate the prediction for numerical value of viral particle exposure  $N_{exp}$  are presented. The predicted value for  $N_{exp}$  is plotted on the graph at the right. The predicted value is shown using a red diamond, and the range of predicted values are shown using the blue rectangles. A detailed discussion of how the range is established is provided in Methods. Note that there were two sources for the events at the health products shop and the jewelry shop<sup>23</sup>, and the estimated respiratory rate is elevated for the fitness classes<sup>22</sup>; these directly alter the  $N_{pred}$ .